Wasit Journal of Engineering Sciences

Journal homepage: https://ejuow.uowasit.edu.iq

Flow field and heat transfer characteristics in dimple pipe with different shape of dimples

Sajida Lafta Ghashim[1]

Affiliations
[1]Department of Mechanical Engineering,
College of Engineering,
University of Baghdad,
Baghdad, Iraq.

Correspondence
Sajida Lafta Ghashim
Sajda_lafta@yahoo.com

Received
09-January-2024
Revised
13-February-2024
Accepted
27-March-2024

Doi:
10.31185/ejuow.Vol12.Iss2.515

Abstract

In this work, a numerical study of a thermal performance of water flow inside a dimpled pipe. The effect of three types of dimples (circular, square and rhombus) studied in the numerical simulation. A commercial program called ANSYS was used to model the flow through a circular pipe .The three-dimensional governing differential equations of mass, momentum, and energy were used together with the ($K-\varepsilon$) model to evaluate the impact of dimples on a turbulent flow and the velocity field. The study was carried out in the Reynolds number (Re) range (2500–15000). The research results demonstrate that the presence of a dimple on the pipe surface greatly increases the rate of heat transmission and the friction factor compared to a normal smooth pipe. Also, the numerical study demonstrated that the Nusselt number (Nu) in case of circular dimples at diameter (4 , 6 and 8) mm was (22, 28 and 43) % greater than the smooth surface. It is discovered that the improved pipe with circular dimples have a benefit for increased heat transmission efficiency compared with the square and rhombus dimples. Additionally , circular dimples have the ability to supply the lowest friction factor (*f*) when compared to other types of dimple. The pipe with circular dimples with D= 4mm , at Reynolds number 2500 provided the largest thermal performance criterion (PEC) value about 1.44.

Keywords: Dimpled pipe ; heat transfer coefficient ; Pressure drop ; dimple size ; performance factor

الخلاصة:

يتضمن هذا العمل دراسة عددية للأداء الحراري لجريان الماء داخل أنبوب ذو ندب. تأثير ثلاثة أنواع من الندب (الدائرية والمربعة والمعينية) تم دراستها بالحل العددية.تم استخدام برنامج يسمى ANSYS لنمذجة التدفق خلال أنبوب دائري. تم استخدام المعادلات التفاضلية الحاكمة ثلاثية الأبعاد للكتلة والزخم والطاقة مع نموذج ($K-\varepsilon$) لتقييم تأثير الندب على الجريان المضطرب ومجال السرعة. أجريت الدراسة في نطاق أرقام رينولدز (2500-15000). أظهرت نتائج البحث أن وجود الندب على سطح الأنبوب يزيد بشكل كبير من معدل انتقال الحرارة وعامل الاحتكاك مقارنة بالأنبوب الأملس العادي. كما بينت نتائج البحث أن رقم نسلت في حالة الندب الدائرية بأقطار (4، 6، 8) ملم ازداد بنسبة (22، 28، 43)% مقارنة بالسطح الأملس. ايضا لوحظ أن الأنابيب ذات الندب الدائرية لها فائدة في زيادة كفاءة نقل الحرارة مقارنة بالندب المربعة والمعينية. بالإضافة إلى ذلك، تتمتع الندب الدائرية بالقدرة على توفير أقل عامل احتكاك مقارنة بأنواع الندب الأخرى. الأنبوب ذو الندب الدائرية بقطر = 4 ملم عند رينولدز 2500 قدم أكبر قيمة للأداء الحراري حوالي 1.44.

1. INTRODUCTION

In numerous regions of the world, improving heat transfer by changing the surface of the tubes is a widely used technique. To improve the surfaces of tubes and channels, grooves, dimples, flutes, or corrugations are inserted within and outside of the surfaces[1] [2].Dimples can offer enhanced heat transfer capabilities equivalent to eddy current generators, which encourages flow zones near walls and lowers pressure loss. Because of its advantage in having a high surface area-to-volume ratio and a significant convective heat transfer coefficient, the dimples are one of the most useful forms for enhancing heat transfer in industrial applications . Numerous research projects have investigated the effects of dimple forms, such as circular, ellipse, and triangular [3] [4][5] [6][7] and [8]. The results show that the rate of heat transfer performance for dimple tubes is higher than that of smooth tubes.

2. LITERATURE REVIEW

In [9] studied experimental and numerical how dimples affect the velocity distribution and turbulent motion, in a double heat exchanger .The Reynolds number range for studies using water as the operating fluid was covered at (500 to 8000), while the range of experiments using water/glycol solution was(150 to 2000). According to the results of the simulation, dimples disrupt and mix boundary layers and produce secondary flows that raise the turbulence level .When compared to an equivalent smooth tube, it was discovered that the improved heat transmission was over 200%. When the Reynolds number ranged from 3500 to 4500 for water, the highest thermal performance (PEC = 1.55) was obtained. [10] investigated experimental work to improve heat transfer through modifying the wall surface of the heat exchanger tubes. The modification was made through inserting a protruding sheet metal surface with a specified shape within the tube and attaching it to the wall surface of the tube. The investigation was carried out using the following parameters: Reynolds number of (6000 to 35000) , stream -wise spacing (10, 20, 30, and 40), span -wise spaced (10, 20, 30, and 40). The experimental results show that the heat capacity for performance and friction factor are much higher with the protrusion on the heat exchanger wall compared to the conventional heat exchanger tube. The heat transmission and pressure loss of R-134a through a condensation process in a dimpled pipe are examined by [11]. The test section consist of a horizontal two concentric tubes the R-134a flowing in the inner tube and water flowing in the annulus. Smooth and dimpled tubes are used as the inner tubes for the test runs. The experiment tests are conducted with mass fluxes of 300 to 500 kg/m^2 .s, heat fluxes of 10 to 20 kW/m^2, and saturation temperatures of 40 to 50 °C. It has been found that a dimpled tube has a higher heat transfer coefficient and pressure drop than a smooth tube. Additionally, compared to a smooth tube, the dimpled tube raises the Nusselt number by 1.3-1.4 times as the Reynolds number rises. [12] numerically studied thermal performance of flow in tube with dimples and protrusions on tube surfaces . The numerical simulations used the K- ε turbulence model with Reynolds number ranging from (5000 to 30000).To demonstrate the processes for improving heat transfer efficiency , the local streamlines, contour of velocity, contour of temperature, Nusselt number and friction factor were displayed. The results show that when protrusion depth increases, the Nusselt number and friction factor increase while the thermal performance criterion decreases. Additionally, it is discovered that as protrusion pitch increases, the friction factor initially decreases and subsequently increases.[13] conducted a numerical study a semi-dimple pair on the fin and tube heat exchanger .The diameter, attack angle, and placement of the semi-dimple are the parameters stuided. The thermal performance of the fin with -dimples is compared to that of the plain fin and the fin with existing dimples in the Reynolds number of (813 to 4019).The outcomes show that the present semi-dimple has the largest pressure loss and coefficient of heat transfer. Also, the pair of semi-dimples has a goodness factor that is approximately (33–37%) higher than the dimples and (15-20%) more than the clear fin. [14] numerically examined heat transfer characteristics in tube with slotted dimples and compared with spherical/elliptical dimples. Results showed that the improved tube with slot dimples is found to have a higher rate of heat transfer than the elliptical or spherical/ dimple tube because the slot dimples created more swirling flow, better fluid mixing, and more flow restriction. Furthermore, the slot dimples caused the boundary layer to collapse, intensify flow mixing, and create periodic impinge flows, significantly enhancing thermal-hydraulic performance. The greatest overall thermal performance evaluation criterion value of 2.02 was produced by the improved tube with slot dimples with diameter 1.5 mm, pitch 30 mm, and Reynolds number 5000.[15] To enhance heat transmission in the solar water heating system, dimple pipes are used in a numerical investigation. Pitch-to-dimple diameter ratio , number of dimples, and mass flow rate are varied during simulation. The ideal number of control volumes is found to be 2.2 million in order for the result to be mesh-independent. The difference in error between the CFD simulation and the experimental result is less than 10% .The dimples on the tube disrupt fluid flow and reduce the hydraulic diameter, thus increasing the collector's efficiency and rate of heat transfer. For the dimpled tube, a maximum increase in the Nusselt number of 2.5 was noted. [16] examined the heat transfer enhancement and friction loss with flow field structures over different types of dimple diameter in turbulent three dimensional tube with using K- ε turbulent model. Three different tube dimpling arrangements with water as the operating fluid are studied over a range of Reynolds number from (1500 to 24000). The findings of the numerical analysis demonstrated that the middle cross-sectional direction of the pipe with and without dimples had symmetric flow fields. Additionally, there are small vortices and eddies in the flow close to the dimples, which is chaotic. According to the outcomes, the temperature variations in the dimple tube with a 2mm diameter at low flow rates of 0.56 L/min was larger by 26.8%, 10.57%, and 3.68%, respectively, than that in smooth pipes, dimple tubes 0.75, and 1.5mm. Numerical exploration of numerous dimple designs with a combination of twisted tape and corrugated tubes by [17]. Water is used as the working fluid within the boundary condition of heat flux applied on pipe wall surfaces. The dimples utilized in this investigation have dimensionless diameters of (0.09, 0.18, 0.27, and 0.36) and the diameter of the corrugation configuration is 1 mm. The Reynolds number used for the numerical simulations is between (1500 and 14000). The findings indicate that when the dimple diameter develops, the Nu number improves. [18] used the K- ε model to conduct a numerical investigation of the heat transmission and flow characteristics in the cross combined dimple pipe. On the surface pipe, a cross-combined dimple is formed by the combining of two ellipsoidal dimples. They are all equally spaced apart in the axial direction. The findings show that as compared to

a single ellipsoidal dimple tube at the specified operating conditions, the heat transfer index, friction factor, and performance evaluation criteria all significantly increase.
Despite the fact that previous research demonstrated that the insertion of dimples or protrusions on tubes may provide a realizable heat transfer improve . But a small number of studies concentrate on the simultaneous increased heat transmission and lower pressure. In this study, focusing more attention to the type or size of the dimple that increases the rate of heat enhancement with low pressure drop. Outcomes of the flow in pipes with and without dimples, such as pressures, velocities, temperatures, and friction factors have been recorded.

3. COMPUTATIONAL SPECIFICATIONS

3.1 Physical Model

The current study examines the thermal properties of flow in the pipe with dimples. **Fig.1** depicts the geometrical design of a smooth circular pipe with inner diameter of D_i= 25 mm , outer diameter of D_o= 28mm and a length of L= 600 mm and the pipe wall is made of copper with uniform heat flux of 1000 W put on the outside walls of the outer diameter . **Fig.1** to **Fig.4** show the smooth pipe and the dimple pipes are manufactured. Pipe with circular dimple using three dimensions of diameter are (D= 4, 6 ,and 8) mm .Also using another type of dimples square, and rhombus with D =6 mm . The various dimpled pipes have the same dimple pitch P= 25mm and equally spaced out on the surface of the pipe at the same perimeter. For all studies cases, the initial water temperature is fixed to 303 K.

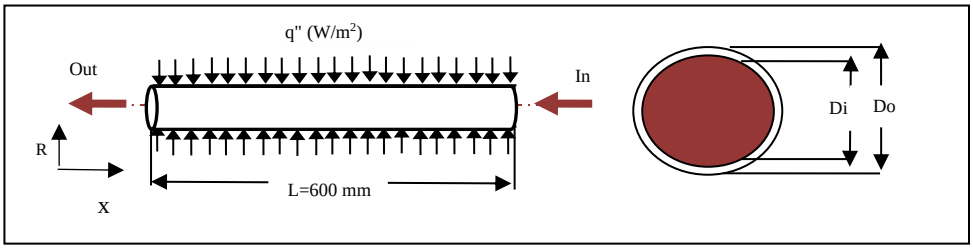

Fig.1 Smooth pipe sketch with dimensions

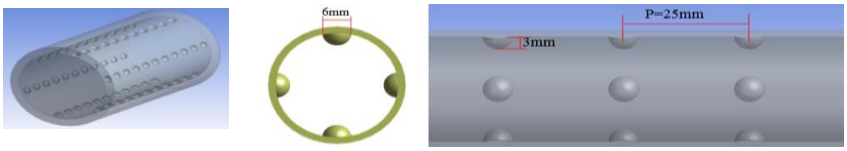

(a) Isometric section (b) Elevation section (c) Side view section

Fig.2 Circular dimple pipe (D=6mm)

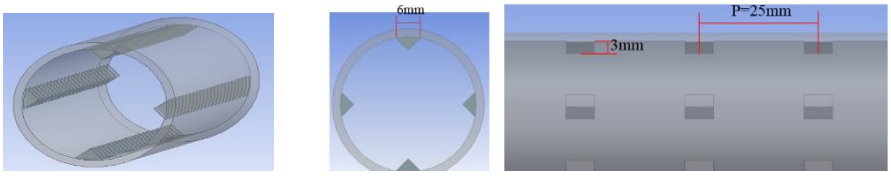

(a) Isometric section (b) Elevation section (c) Side view section

Fig.3 Rhombus dimple pipe (D =6mm)

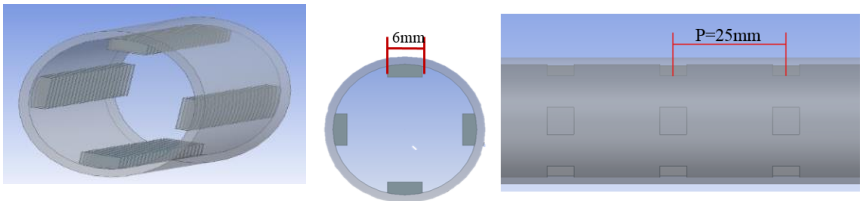

(a) Isometric section (b) Elevation section (c) Side view section

Fig.4 Square dimple pipe (D =6mm)

3.2 Governing Equations

The fluid flow through a pipe is considered to be three-dimensional, turbulent, incompressible, and to maintain a constant property. The (K − ε) turbulence model is used in this investigation [19]:

- Continuity equation

$$\frac{\partial}{\partial x_i}(\rho u_i) = 0.0 \quad (1)$$

- Momentum equation

$$\frac{\partial}{\partial x_j}\left(\rho u_i u_j\right) = -\frac{\partial P}{\partial x_i} \pm \rho g + \frac{\partial}{\partial x_j}\left[\mu\left(\frac{\partial u_i}{\partial x_j} + \frac{\partial u_j}{\partial x_i} - \frac{2}{3}\delta_{ij}\frac{\partial u_l}{\partial x_l}\right)\right] + \frac{\partial}{\partial x_j}\left(-\rho\acute{u}_i\acute{u}_j\right) \quad (2)$$

- Energy equation

$$\frac{\partial}{\partial x_i}(\rho T u_i) = \left\{\frac{\partial}{\partial x_j}\left[c_p\left(\frac{\mu}{pr} + \frac{\mu_t}{\sigma_t}\right)\frac{\partial T}{\partial x_j}\right]\right\} \quad (3)$$

-Turbulence modeling

-Turbulent kinetic energy

$$\frac{\partial}{\partial x_i}(\rho u_i K) = \frac{\partial}{\partial x_j}\left[\left(\mu + \frac{\mu_t}{\sigma_k}\right)\frac{\partial K}{\partial x_j}\right] + \left(G_K - \rho\varepsilon\right) \quad (4)$$

-Turbulent dissipation rate

$$\frac{\partial}{\partial x_i}(\rho u_i \varepsilon) = \frac{\partial}{\partial x_j}\left[\left(\mu + \frac{\mu_t}{\sigma_\varepsilon}\right)\frac{\partial \varepsilon}{\partial x_j}\right] + \left(\frac{c_{\varepsilon 1} G_K \varepsilon}{K} - \frac{c_{\varepsilon 2}\varepsilon^2 \rho}{K}\right) \quad (5)$$

Where:

$$G_k = -\rho\overline{\acute{u}_i\acute{u}_j}\frac{\partial u_j}{\partial x_i} \quad (6)$$

$$\mu_t = C_\mu \rho f_\mu \frac{K^2}{\varepsilon} \quad (7)$$

The constants of (K − ε) models showed in the above equations are the same as those indicated in [19][20] , C_μ = 0.09, σ_k = 1.0, σ_ε = 1.3, $C_{\varepsilon 1}$ = 1.44 and $C_{\varepsilon 2}$ = 1.92

3.3 Boundary Conditions and Data Reduction

- Uniform temperature and velocity profiles at the circular pipe entrance are assumed as follows:

$$v = 0 \ , w = 0 \ , u = u_{in} \ , T = T_{in} \quad (8)$$

- The entrance profile for the turbulent kinetic energy and turbulent dissipation rate are calculated from:

$$K_{in} = 0.03\, {u_{in}}^2 \quad , \quad \varepsilon_{in} = C_\mu \frac{{K_{in}}^{3/2}}{0.03R} \quad (9)$$

- The boundary conditions at exit as follows:

$$\frac{\partial u}{\partial x} = \frac{\partial v}{\partial x} = \frac{\partial w}{\partial x} = 0 \quad , \frac{\partial T}{\partial x} = 0 \quad , \quad \frac{\partial P}{\partial x} = 0 \quad (10)$$

$(K - \varepsilon)$ model boundary condition at exit as follows: $\frac{\partial K}{\partial x} = \frac{\partial \varepsilon}{\partial x} = 0$ (11)

- All velocity components are zero at the walls (no-slip condition) hence: $u = v = w = 0$ (12)

The boundary condition of the for turbulence models is: $K = 0 \quad , \quad \frac{\partial \varepsilon}{\partial r} = 0$ (13)

For the constant heat flux, the boundary condition will be as follows: $\frac{\partial T}{\partial r} = \frac{q''}{\lambda}$ (14)

The ratio of inertial force to viscous force is represented by the Reynolds number. The Reynolds number is written as follows:[21]:

$$Re = \frac{\rho\, u_{in} D_i}{\mu} \quad (15)$$

The coefficient of heat transfer is defined as [22]:

$$h_x = \frac{q''}{(T_{wall(x)} - T_{bulk(x)})} \quad (16)$$

where T_{wall} and T_{bulk} are wall temperature and temperature of fluid , q'' is total heat flux rate.

$$T_{bulk} = \frac{\int_0^R uT(2\pi r)dr}{\int_0^R u(2\pi r)dr} \quad (17)$$

The amount of convective heat transport is measured by the Nusselt number. The Nusselt number is described as[23]:

$$Nu_x = \frac{h_x D_i}{\lambda} \quad (18)$$

$$\mathrm{Nu} = \frac{1}{L}\int_0^L Nu_x dx \quad (19)$$

The friction factor, as defined by Fanning factor , is used, and it is as follows:

$$f = \frac{\Delta P}{\left(\frac{L}{D_i}\right)\left(\frac{\rho u^2 in}{2}\right)} \quad (20)$$

Where L is the length of the test section, ΔP is the pressure differential for the test section, and u_{in} is the mean inlet velocity.

Thermal performance criterion (PEC) that takes into account the friction loss and the heat transfer improvement and proposed by Gee and Webb [24] computed as follow:

$$\text{PEC} = \frac{Nu_{\text{with dimple}} / Nu_{\text{without dimple}}}{\left(f_{\text{with dimple}} / f_{\text{without dimple}}\right)^{1/3}} \quad (21)$$

3.4 Mesh Simulation of Flow Configuration

In this study, the governing deferential conservation equations of continuity, momentum, and energy are discretized using the finite volume approach. ANSYS 20 is used to solve each governing equation. The pressure equation was solved using the second order discrete technique, and the pressure velocity coupling problem is resolved using a straightforward approach [25]. The second-order upwind discrete technique is utilized to solve the momentum, turbulent kinetic energy, and turbulent dissipation rate. The (K − ε) turbulence model with an enhanced wall function are used [26]. The convergence criteria for all variables are 10^{-8}. **Fig.5** and **Fig.6** illustrates the mesh in smooth and dimple pipes Additionally, in order to use the upgraded wall functions in the simulations, the grids domain needs to undergo repeated debugging to make sure that the wall y-plus value is close to or below 1.0.

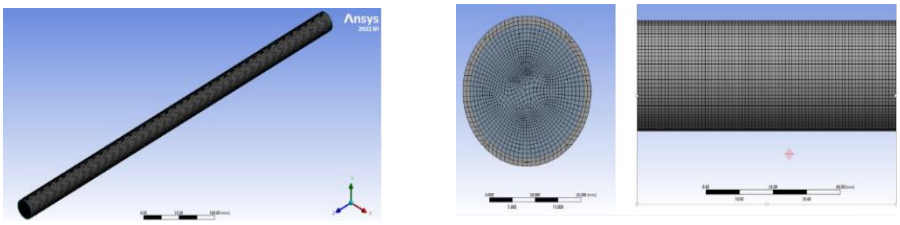

(a) Isometric section (b) Elevation section (c) Side view section

Fig.5 Grid patterns of pipe without dimples

(a) Circular dimple (b) Rhombus dimple (c) Square dimple

Fig.6 Grid patterns of various dimples (a) Circular dimple (b) Rhombus dimple (c) Square dimple

3.5 Validation

The validity of the solution methodology used in this study is shown by comparing the simulation results with the experimental data currently available, which was obtained using the Dittus-Boelter equation, the Gnielinski equation, for the Nusselt number and the Petukhov equation, and the Blasius equation for the friction factor to the turbulent flow in the smooth tube [10] .

The Dittus- Boelter equation: $Nu = 0.023 \times Re^{0.8} \times Pr^{0.4}$ (22)

The Blasius equation: $f = 0.3164 \times Re^{-0.25}$ (23)

The Gnielinski equation : $Nu = 0.03277 \times Re^{0.742} \times Pr^{0.4}$ (24)

The Petukhov equation : $f = 0.6165 \times Re^{-0.317}$ (25)

Fig.7 displays a comparison of smooth pipe. In **Fig. 7a** the numerical results of Nusselt number are compared with empirical equations. The numerical outcomes for a smooth pipe are seen to match well with correlations data, the results show that the maximum and minimum deviations between the present results and the Dittus- Boelter equation are 5.7 % at Re = 2500 and 14.2% at Re= 12000, respectively. Also , the present work results are in good agreement with Gnielinski equation , the minimum deviations 5% and the maximum is 19%. In **Fig.7b**, shows the comparison between the results of present work and empirical equations for friction factor .Obviously, the deviations between the present results and the correlations is very high at low Reynolds number at value 2500 and these deviations is decreased to 4.3% with increased Reynolds number to Re = 12000 .

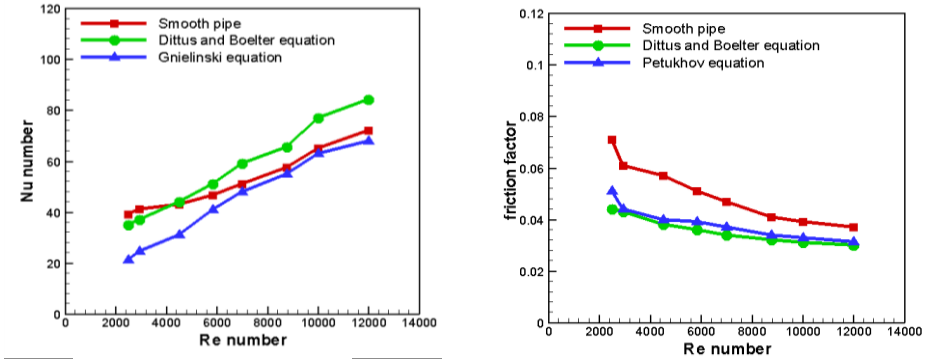

(a) Nusselt number (b) friction factor

Fig.7 Comparison of the numerical results with the empirical equations

Also, in **Fig.8** describes the comparison between the present results and results from [16] in the pressure in the smooth pipe during working conditions, the mass flow was 0.56 L/min, and inlet temperature 313.15 K. It is evident that the relative maximum variation in pressure between the two results from inlet to outlet flow is 5% to 9%.

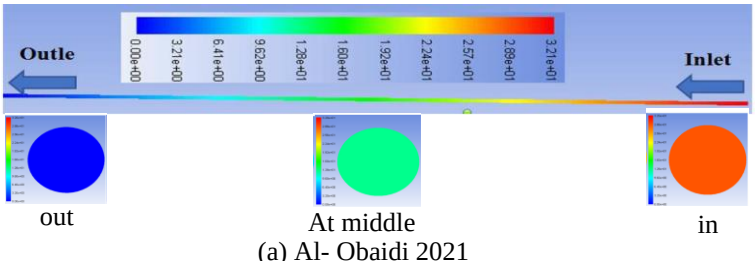

(a) Al- Obaidi 2021

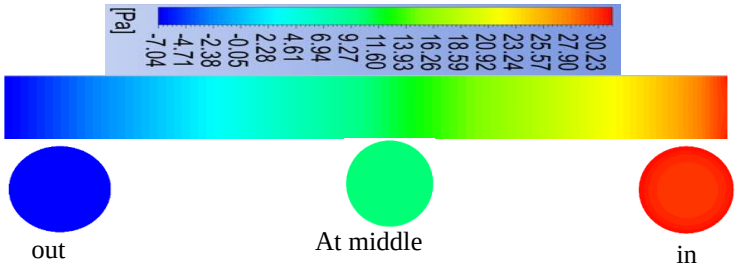

(b) Present work

Fig.8 Validation of present work by comparison the pressure with Al- Obaidi 2021

A comparison between the outcomes of [16] and the current numerical study is shown in **Fig.9** . In the Al-Obaida 2021 , test section, the pipe has a diameter of 11.08 mm, the length is 1920 mm, and the diameter of the dimple is 0.75 mm. The numerical results and[16] reasonably agreement as can be shown.

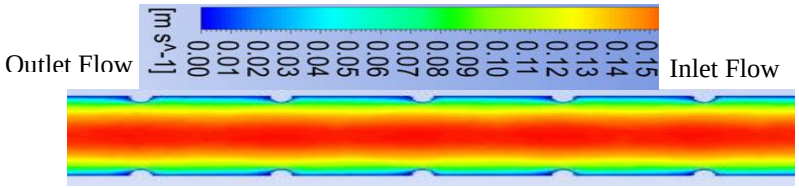

(a) Present work

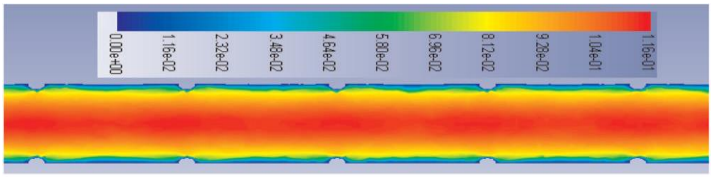

(b) Al- Obaidi 2021

Fig.9 Validation of present work by comparison the contour of velocity with Al- Obaidi 2021

4. RESULTS AND DISCUSSIONS

In **Fig.10**, the numerical findings of the contour of temperature comparison of smooth and circular dimple pipe at power= 1000W. Along the direction of movement, the fluid's average temperature increased. Figure displays the temperature distributions for dimpled pipes of various diameters. In comparison to the clear pipe's temperature field, the dimple pipe's temperature field is changed and deformed by the dimples, becoming increasingly uniform along the direction of the flow. The average temperature of the dimpled pipe with the bigger diameter is higher. Additionally, it is clear that when the diameter of the dimple at the pipe wall increases, the temperature inside the pipe rises along with it.

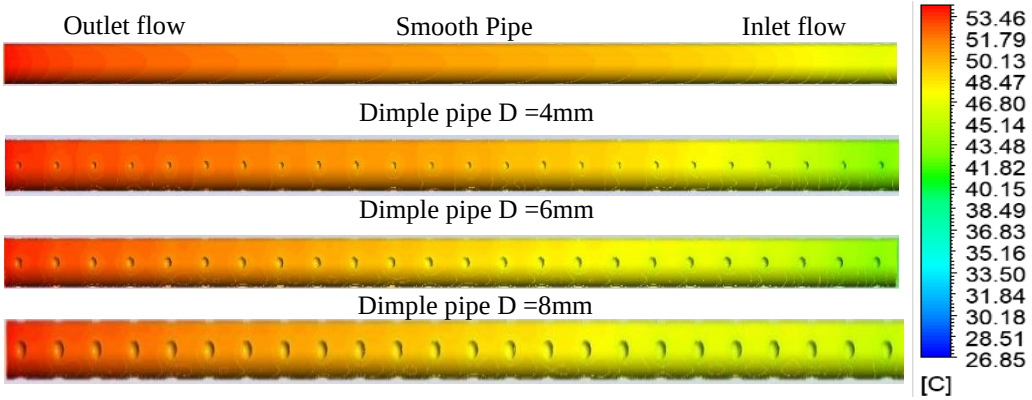

Fig.10 Contour of temperature comparison of smooth and circle dimple pipe at Re number = 2920 , po= 1000W

The temperature variations for circular , square and rhombus dimpled pipes are shown in **Fig.11.** The temperature begins to decrease at the input and in the output of the pipe increase. Additionally, the average temperature of circular dimple is larger than square and rhombus dimpled pipes.

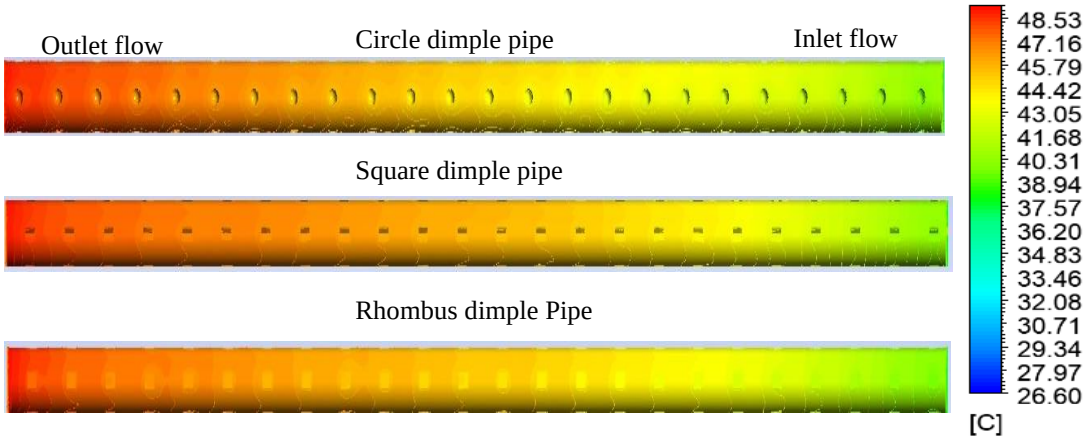

Fig.11 Contour of temperature comparison of circle, rhombus and square dimple pipe at Re number = 2920 , D=6 mm and po=1000W

Fig.12 and **Fig.13** present the of axial and radial pressure distribution for different dimpled pipes for Re=2920 and power =1000 W. As the pipe length developed, the fluctuations in pressure became less noticeable. The input pipe zone has a higher pressure value, whereas the output pipe region has a lower value. From this figure, several observations may be observed. The higher value of pressure occurs at the distance between the center and near-wall pipe. Additionally, because of this reign's low velocity value, the pressure is lower towards the pipe wall. Furthermore, it should be noted that when the diameter of the dimple at the pipe wall increases, the pressure inside the pipe additionally increases. This occurred as a result of increased resistance in the pipe. Furthermore, in the same pipe with square and rhombus dimpled can significantly increase the pressure drop compared to a smooth

pipe. Due to the rise in resistance flow caused by a dimple, there has been a large increase in pressure drop a similar observation was show by [16].

Fig.14 shows the velocity amount fluctuations in pipes with and without dimples of various diameters and types. It is evident that as the diameter of a circular dimple develops, it also increases the average velocity, with a relatively small velocity occurring downstream of the dimple. Due to the blockage effect, the larger diameter may supply higher velocity, which causes the velocity to increase as the diameter is increased. This graphic also clearly illustrates the scales and locations of recirculation flows. It can be seen that the streamlines are distorted by dimples, particularly in the region close to the wall, and that the magnitude of the recirculation flow considerably decreases as the diameter decreases. As a result, it is reasonable to assume that the fluid will mix more effectively when large-scale vortices of greater diameter are available.

Additionally, **Fig. 14** displays the velocity distribution across three dimpled tubes (circular, square, and rhombus). It is evident that along the entire dimpled tube, the local velocity increased upstream of the dimples and decreased downstream along the flow direction. The fluid movement on and away from the pipe wall caused by the velocity fluctuation helped the boundary layer develop and hence enhanced the efficiency of heat transfer. It is important to note that in diameter of 6 mm, the vortices in circular dimple pipes are larger in size and stronger than those in square and rhombus examples. As a result, it is reasonable to assume that the fluid will mix better in the circular dimple pipe case.

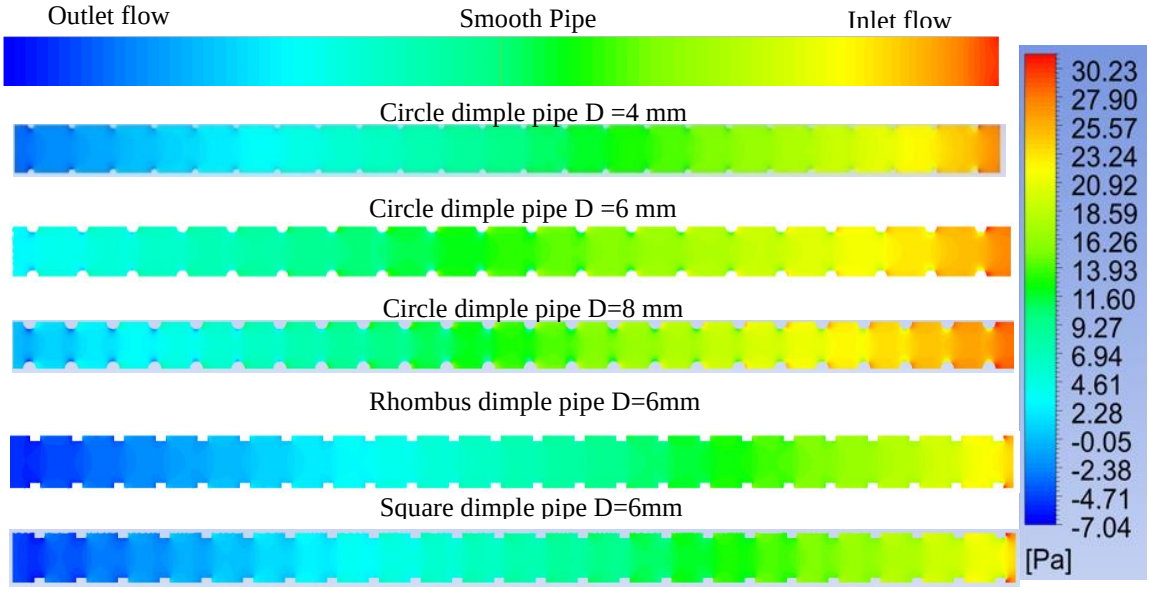

Fig.12 Contour of axial pressure distribution of smooth pipe and dimple pipe at po=1000W and Re=2920

Fig. 15a shows the influence of various circular dimple diameters on Nusselt number and Re number. The Nusselt number decreases as Re increases and D decreases. Obviously, D = 4 mm has the smallest Nusselt number while D = 6 mm has a rather high Nusselt number. D = 8 mm gives the largest Nusselt number because of the significant the obstruction and separation. Additionally, compared to smooth pipes, the magnitude of the Nu number for circular dimples of all diameters is larger. That's because of the effect of mixing and a secondary vortex that forms close to the surfaces of the dimples. For varying circular dimple diameters, friction factor increases with decreasing Re number is depicted in **Fig.15b**. The friction factor increases as the D is raised, which is to be predicted. The main reason of the rapidly rising friction factor at larger D is high flow impingement, which led to a greater pressure drop.

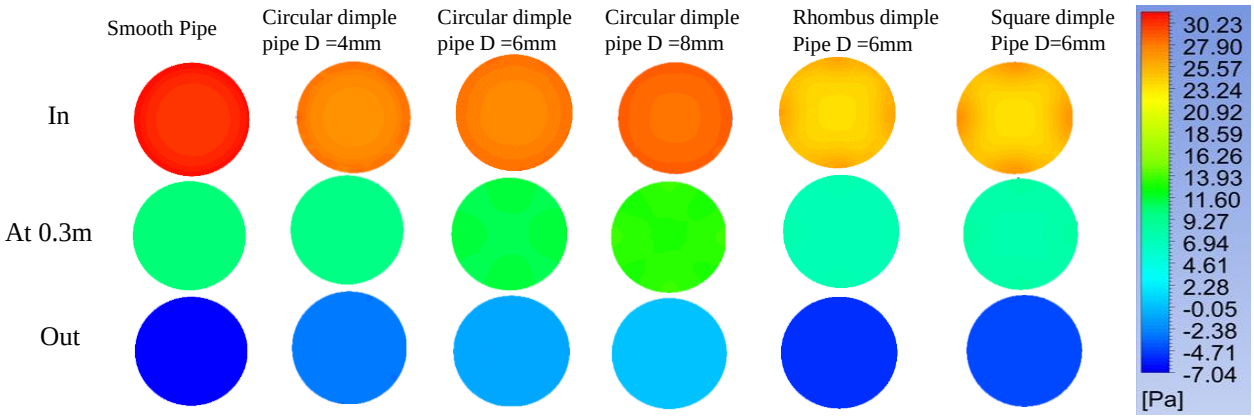

Fig.13 Contour of radial flow directions of pressure of smooth pipe and dimple pipe at po=1000W and Re=2920

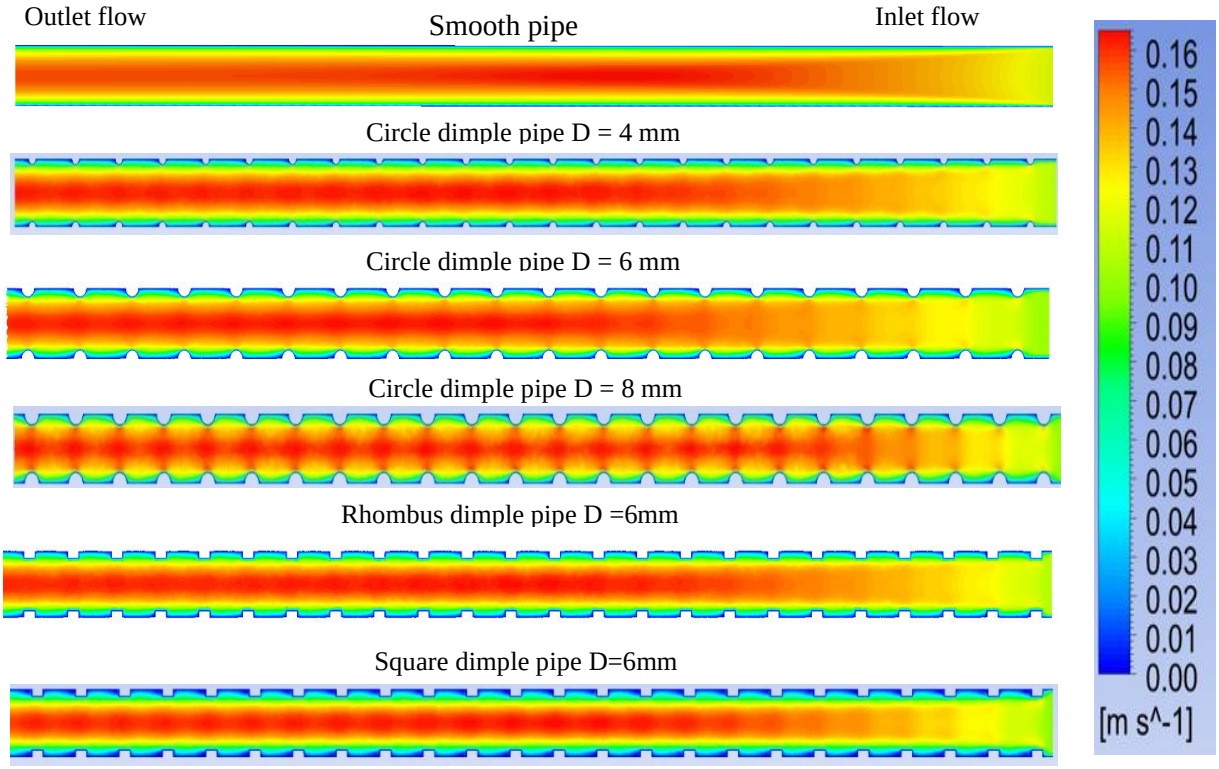

Fig.14 Contour of velocity comparison of smooth pipe and dimple pipe at po=1000W and Re=2920

For different kinds of dimple, Nu number is shown in **Fig.16a** with variable Re number. As Re increases, the Nu number rises. The improved pipe with circular dimples is found to have a greater rate of heat transfer than the pipe without a dimple or the pipe with square or rhombus dimples because the circle dimples caused more swirling flow, better fluid mixing, and more flow obstruction. The circular dimples significantly improved thermal-hydraulic performance by destroying the boundary layer and causing strong flow mixing and periodic impinge flows. **Fig.16b** demonstrates the friction factor for several types of dimple. The trend of the friction factor first decreases sharply and then slightly with an increase in Re number . Additionally, circular dimples that produced the lowest friction factor in comparison to other types, this tendency is mainly due to the circular dimple that successfully decreases flow recirculation and low pressure loss.

Fig. 17 displays the thermal performance criterion PEC with Re number for various circular dimple diameters D. The PEC declines with increasing Re and D similar results show by [9]. The highest PEC is achieved by the D = 4 mm in all tests of Re number, with values ranging from 1.19 to 1.44.

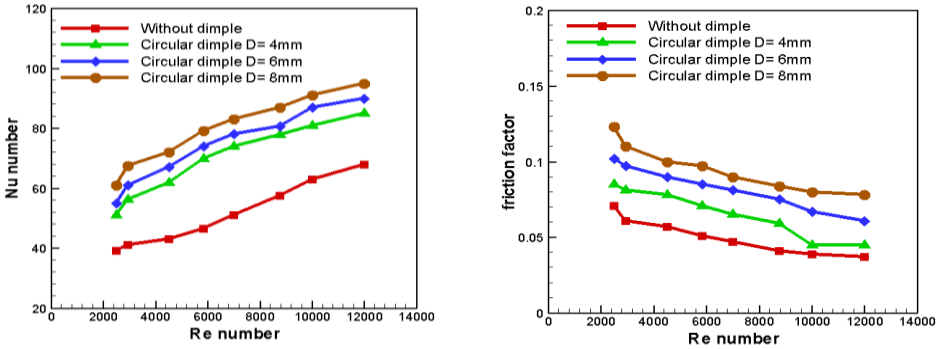

(a) Nusselt number (b) friction factor

Fig.15 Impact of diameter of circular dimple on Nu number and friction factor

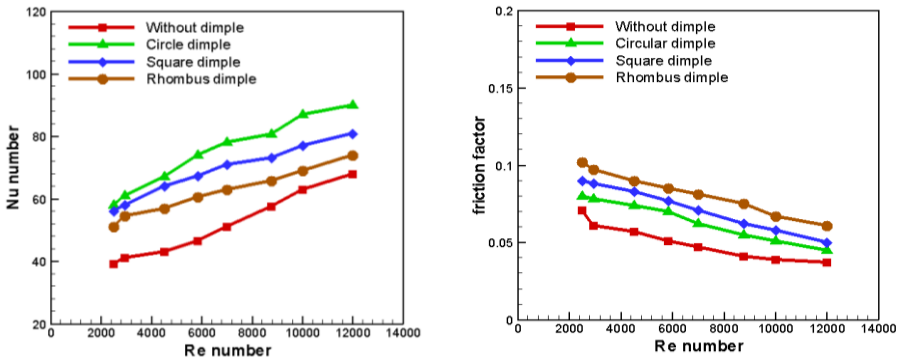

(a) Nusselt number (b) friction factor

Fig.16 Impact of different kinds of dimple on Nu number and friction factor

Additionally, the smallest value of PEC at D = 8 mm and a PEC value between 1.25 and 1.11. The impact of various dimple types on the thermal performance factor, as shown in **Fig.18**. With an increase in Reynolds number, the PEC reduces. When the Re number rises from 4000 to 6000, the value of thermal PEC for circular and square dimples rises. When the Re number rises to 120000, the value of thermal PEC reduces. The value of PEC decreases for case rhombus dimple as the Re number rises. Additionally, the lower and upper PEC values for circular dimples are around 1.35 and 1.12.

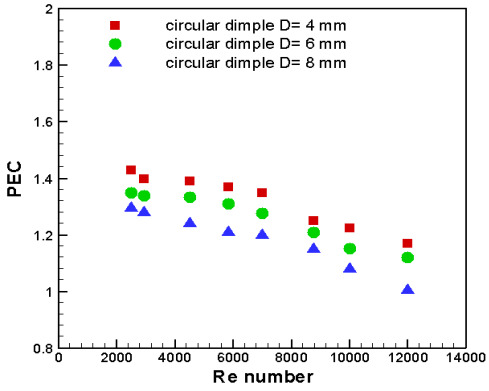

Fig.17 Impact of diameter of circular dimple on thermal performance criterion

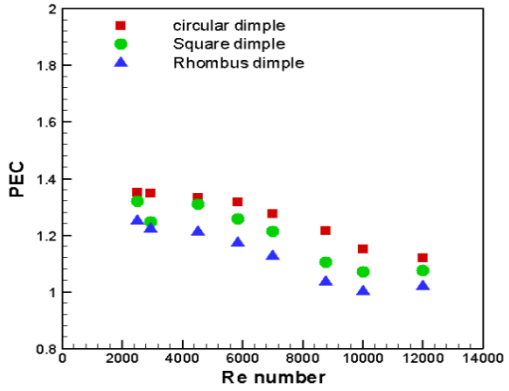

Fig.18 Impact of types of dimple on thermal performance criterion

5. CONCLUSIONS

In this research, a three-dimensional, turbulent flow, and steady-state numerical simulation were used to examine the impact of circular dimple diameters and dimple types on the flow structure and heat transfer properties in a pipe. The primary result can be summarized in as follows:

1. The velocity distribution varies as the diameter of the dimple increases, particularly in the pipe sections close the dimples.

2. The pressure drop in the pipe is reduced as the length of pipe increases with a higher pressure value in the entrance of the pipe.
3. As the dimple diameter developed, the Nusselt number in dimple pipe increased by 22% at D=4 mm, 28% at D=6 mm, and 43% at D=8 mm at Re=12000 as compared to smooth pipe.
4. At low Reynolds number value 2500, dimple shape has a more obvious impact on friction factor. The friction factor increased by 35% at rhombus dimple, 27% at square dimple and 8% circular dimple.
5. At each condition of operation, the enhancement of heat transfer was more than the enhancement of pressure drop, resulting to a higher PEC.
6. In comparison to the rhombus and square dimpled pipes, the circular pipe dimple has higher thermal performance criterion because the intensity and extent of the recirculation flow is much reduced.
7. Circular dimple with D= 4mm showed higher performance PEC in the Re number 2500.
8. When compared to rhombus and square dimples, the circular dimple showed the highest performance (PEC = 1.35) at Re number 2500 with D= 6mm .

REFERENCES

[1] A. Samad, K.-D. Lee, and K.-Y. Kim, "Multi-objective optimization of a dimpled channel for heat transfer augmentation," Heat Mass Transf., vol. 45, no. 2, pp. 207–217, 2008, doi: 10.1007/s00231-008-0420-6.

[2] N. F. Hussein and A. S. Mahmood, "Enhancing heat transfer in tube heat exchanger by inserting discrete twisting tapes with different positions," J. Eng., vol. 25, pp. 39–51, Jul. 2019, doi: 10.31026/j.eng.2019.08.03.

[3] H. S. Yoon, S. H. Park, C. Choi, and M. Y. Ha, "Numerical study on characteristics of flow and heat transfer in a cooling passage with a tear-drop dimple surface," Int. J. Therm. Sci., vol. 89, pp. 121–135, 2015, doi: https://doi.org/10.1016/j.ijthermalsci.2014.11.002.

[4] F. Zhou and S. Acharya, "Experimental and computational study of heat/mass transfer and flow structure for four dimple shapes in a square internal passage," J. Turbomach., vol. 134, Jan. 2009, doi: 10.1115/GT2009-60240.

[5] G. Xie, J. Liu, P. M. Ligrani, and W. Zhang, "Numerical predictions of heat transfer and flow structure in a square cross-section channel with various non-spherical indentation dimples," Numer. Heat Transf. Part A Appl., vol. 64, no. 3, pp. 187–215, Aug. 2013, doi: 10.1080/10407782.2013.779485.

[6] K.-Y. Kim, M. A. Moon, and H. M. Kim, "Shape optimization of inclined elliptic dimples in a cooling channel," J. Thermophys. Heat Transf., vol. 25, pp. 472–476, Jul. 2011, doi: 10.2514/1.55158.

[7] J. Pandit, M. Thompson, S. V Ekkad, and S. T. Huxtable, "Effect of pin fin to channel height ratio and pin fin geometry on heat transfer performance for flow in rectangular channels," Int. J. Heat Mass Transf., vol. 77, pp. 359–368, 2014, doi: https://doi.org/10.1016/j.ijheatmasstransfer.2014.05.030.

[8] J. Hua, G. Li, X. Zhao, Q. Li, and J. Hu, "Study on the flow resistance performance of fluid cross various shapes of micro-scale pin fin," Appl. Therm. Eng., vol. 107, pp. 768–775, 2016, doi: https://doi.org/10.1016/j.applthermaleng.2016.07.048.

[9] M. Li, T. S. Khan, E. Al-Hajri, and Z. H. Ayub, "Single phase heat transfer and pressure drop analysis of a dimpled enhanced tube," Appl. Therm. Eng., vol. 101, pp. 38–46, 2016, doi: https://doi.org/10.1016/j.applthermaleng.2016.03.042.

[10] P. Kumar, A. Kumar, S. Chamoli, and M. Kumar, "Experimental investigation of heat transfer enhancement and fluid flow characteristics in a protruded surface heat exchanger tube," Exp. Therm. Fluid Sci., vol. 71, pp. 42–51, 2016, doi: https://doi.org/10.1016/j.expthermflusci.2015.10.014.

[11] K. Aroonrat and S. Wongwises, "Experimental study on two-phase condensation heat transfer and pressure drop of R-134a flowing in a dimpled tube," Int. J. Heat Mass Transf., vol. 106, pp. 437–448, 2017, doi: https://doi.org/10.1016/j.ijheatmasstransfer.2016.08.046.

[12] S. Xie, Z. Liang, L. Zhang, Y. Wang, H. Ding, and J. Zhang, "Numerical investigation on heat transfer performance and flow characteristics in enhanced tube with dimples and protrusions," Int. J. Heat Mass Transf., vol. 122, pp. 602–613, 2018, doi: https://doi.org/10.1016/j.ijheatmasstransfer.2018.01.106.

[13] N. Chimres, C.-C. Wang, and S. Wongwises, "Optimal design of the semi-dimple vortex generator in the fin and tube heat exchanger," Int. J. Heat Mass Transf., vol. 120, pp. 1173–1186, 2018, doi: https://doi.org/10.1016/j.ijheatmasstransfer.2017.11.121.

[14] S. Zhang, Liang , Xie, J. Liang, Zheng , Zhang, W. Wang, Yulin , Chen, and C. Kong, "Numerical investigation of flow and heat transfer in enhanced tube with slot dimples," Heat Mass Transf., vol. 55, no. 12, pp. 3697–3709, 2019, doi: 10.1007/s00231-019-02685-z.

[15] M. R B, R. Moorthy, and R. Ragunathan, "Investigation on influence of dimpled surfaces on heat transfer enhancement and friction factor in solar water heater," J. Therm. Anal. Calorim., vol. 145, May 2020, doi: 10.1007/s10973-020-09746-0.

[16] A. R. Al-Obaidi, "Study the influence of concavity shapes on augmentation of heat-transfer performance, pressure field, and fluid pattern in three-dimensional pipe," Heat Transf., vol. 50, no. 5, pp. 4354–4381, Jul.

2021, doi: https://doi.org/10.1002/htj.22079.
[17] A. Al-Obaidi, J. Alhamid, and F. Hamad, “Flow field and heat transfer enhancement investigations by using a combination of corrugated tubes with a twisted tape within 3D circular tube based on different dimple configurations,” Heat Transf., Jun. 2021, doi: 10.1002/htj.22207.
[18] L. Zhang, W. Xiong, J. Zheng, Z. Liang, and S. Xie, “Numerical analysis of heat transfer enhancement and flow characteristics inside cross-combined ellipsoidal dimple tubes,” Case Stud. Therm. Eng., vol. 25, p. 100937, 2021, doi: https://doi.org/10.1016/j.csite.2021.100937.
[19] M. Rostamani, S. F. Hosseinizadeh, M. Gorji, and J. M. Khodadadi, “Numerical study of turbulent forced convection flow of nanofluids in a long horizontal duct considering variable properties,” Int. Commun. Heat Mass Transf., vol. 37, no. 10, pp. 1426–1431, 2010, doi: https://doi.org/10.1016/j.icheatmasstransfer.2010.08.007.
[20] A. W. Ezzat, N. N. Abdullah, and S. L. Ghashim, “Effect of air bubbles on heat transfer coefficient in turbulent convection flow,” J. Eng., vol. 23, no. 1, pp. 8–28, 2017.
[21] J. P. Holman, Heat transfer, Tenth. 2002.
[22] S. L. Ghashim, “A mathematical analysis of nanoparticles on heat transfer in a circular pipe,” Case Stud. Therm. Eng., vol. 28, 2021, doi: 10.1016/j.csite.2021.101524.
[23] A. W. Ezzat and S. L. Ghashim, “Investigation of optimum heat flux profile based on the boiling safety factor,” J. Eng., vol. 25, no. 4, 2019.
[24] D. L. Gee and R. L. Webb, “Forced convection heat transfer in helically rib-roughened tubes,” Int. J. Heat Mass Transf., vol. 23, no. 8, pp. 1127–1136, 1980, doi: https://doi.org/10.1016/0017-9310(80)90177-5.
[25] S. V. Patankar, Numerical heat transfer and fluid flow, Hemisphere. 1980.
[26] H. K. Versteeg and W. Malalasekera, An introduction to computational fluid dynamics-the finite volume method, Longman gr. 1995.

Nomenclature

C_p	specific heat ,J. kg^{-1}. K^{-1}
$C_{\varepsilon1}$, C_μ & $C_{\varepsilon2}$	turbulent model constants
D	dimple diameter, m
D_i	inner diameter ,m
Do	outer diameter ,m
f	friction factor
K	turbulent kinetic energy ,m^2. S^{-2}
L	length of pipe,m
Nu	Nusselt number
P	dimple pitch, mm
ΔP	Pressure drop, Pa
PEC	thermal performance criterion
Po	electrical power , W
q''	heat flux ,$W.m^{-2}$
r	direction ,m
R	radius of pipe ,m
Re	Reynolds number
T	temperature , ^oC
u,v,w	mean velocity components in R, x, θ directions
$\acute{u}_i\acute{u}_j$	Reynolds shear stress components, , m^2. S^{-2}
x	flow along z-direction in the pipe ,m

Greek symbols

ε	dissipation rate of turbulent kinetic energy , m^2. S^{-3}
λ	thermal conductivity ,W. m^{-1}. K^{-1}
μ	fluid dynamic viscosity , N. s. m^{-2}
μ_t	turbulent viscosity, N. s. m^{-2}
μ_e	effective viscosity , N. s. m^{-2}

Subscripts

i	inner
in	inlet
o	outer
wall	wall
bulk	bulk